Available online at www.sciencedirect.com
ScienceDirect
Trans. Nonferrous Met. Soc. China 32(2022) 1405−1415
Transactions of Nonferrous Metals Society of China
www.tnmsc.cn

Impact strength and structural refinement of A380 aluminum alloy produced through gas-induced semi-solid process and Sr addition

M. HONARMAND, M. SALEHI, S. G. SHABESTARI, H. SAGHAFIAN

School of Metallurgy and Materials Engineering,
Iran University of Science and Technology (IUST), Narmak, Tehran, Iran

Received 16 June 2021; accepted 28 November 2021

Abstract: Semi-solid processing of A380 aluminum alloy was performed by gas induced semi-solid (GISS) process. The effects of argon inert gas flow rate, starting temperature and duration of gas purging as key GISS parameters and also modification with Sr on the structural refinements, hardness and impact strength of GISS alloys were investigated. Microstructural evolution shows that there is an important effect of the pouring temperature and Sr addition on the morphology and size of primary α(A1) in the alloy to change from coarse dendritic to fine globular structure. The best sample which has fine grains of 51.18 μm in average size and a high level of globularity of 0.89 is achieved from a GISS processing of Sr modified alloy in which the gas purging started at 610 °C. The impact strength of the GISS optimized samples ((4.67±0.18) J/cm^2) shows an increase of about 40% with respect to the as-cast sample due to the globular structure and fibrous Si morphology. Moreover, the hardness of the optimized GISS sample ((89.34±2.85) HB) increases to (93.84±3.14) HB by modification with the Sr and GISS process. The fracture surface of Sr modified alloy is also dominated by complex topography showing typical ductile fracture features.

Key words: gas-induced semi-solid process; impact strength; A380 aluminium alloy; globular structure; modification

1 Introduction

Recently lightweight alloys have become outstanding to overcome fuel efficiency and environmental pollution in the automotive industry. A380 aluminium casting alloys have been widely used due to their good castability and weldability, high corrosion resistance and high specific strength [1−4]. Conventionally cast aluminum alloys have dendritic primary α-phase morphology which affects the mechanical properties of casting products. Therefore, it is necessary to change the dendritic morphology of alloys into globular structure. Semi-solid metal processing is the most advanced technique to modify morphology [5]. Semi-solid metal forming employing the rheo-casting has drawn interest in recent years. The most advantage of this process is producing high-quality parts with lower costs [6−10].

The preparation of slurry is crucial for semi-solid metal forming, and how to prepare slurry with spherical grains is an important challenge for researchers all over the world. Strong convection or shearing such as mechanical stirring, electro-magnetic stirring and gas induced semi-solid is often used during the solidification of melt [11]. Gas induced semi-solid (GISS) technique was first investigated by WANNASIN et al in 2006 [12]. It was feasible for this method to refine the primary grains and prepare semi-solid slurry. The GISS process induces vigorous convection to the melt and rapid heat extraction using fine gas bubbles as the medium. It has been proven a simple, economical and efficient process [13−16].

Many studies were conducted to reveal the

Corresponding author: S. G. SHABESTARI, E-mail: shabestari@iust.ac.ir
DOI: 10.1016/S1003-6326(22)65882-5

formation mechanism of globular microstructure which is important for process control to produce semi-solid slurry to obtain favorable rheological properties in order to facilitate the subsequent component forming process [10]. It has long been believed that the non-dendritic particles are developed from the initial dendritic morphology, under dynamic agitating conditions through the following mechanism: (1) dendrite arms break off at their roots due to shear force; (2) dendrite arms melt off at their roots; (3) dendrite arms bend under flow stresses creating boundaries within the bent dendrites followed by complete wetting of high angle, high energy grain boundaries by the liquid phase resulting in ultimate break-up of the dendrites. With increasing the shear time, the fragmented dendrite arms change gradually to spheroids via stages of dendrite growth, rosettes and ripened rosettes [17,18]. However, the recent theoretical analysis of the microstructures reveals that the above mechanism might be only applicable to the case of a simple shear flow with a low shear rate. With increasing shear rate and the intensity of turbulence, the growth morphology changes from dendrites to spheres via rosettes due to the change in the diffusion geometry in the liquid around the growing solid phase [18]. It was found that increasing the shear rate and intensity of turbulence can be attributed to the increased effective nucleation rate because of the extremely uniform temperature and composition fields in the bulk liquid at early stages of solidification [19].

Eutectic modification is also a usual chemical refinement method applied in the aluminium–silicon based alloys to improve mechanical properties through structural refinement of the brittle eutectic silicon phase. Addition of strontium in aluminum alloys results in a transformation of the eutectic silicon morphology from a coarse plate-like structure to a well-refined fibrous structure [20,21]. Many possible mechanisms of chemical eutectic modification have been studied in the literature, some of them related to eutectic nucleation, and others to eutectic growth. However, there is still no commonly accepted understanding of the mechanisms that allow the microstructure to change [22].

Most of the mechanical properties reported for cast Al−Si alloys are related to tensile testing. As this test is highly sensitive to additions of alloying elements to the alloy and considerable scatter is usually observed in the results, the test results are not a strong function of silicon morphology. It has been found that the impact testing is extremely sensitive to the addition of alloying elements and to silicon morphology, thus this test was selected in this study. According to previous studies [23], impact strength is the most sensitive of all the mechanical properties to silicon content for alloy compositions containing 3%−15% Si. In this work, the impact behavior of GISS and Sr-modified alloys will be investigated with reference to the as-cast conditions.

There are some researches which have focused on the microstructural change caused by gas-induced semisolid process [6], but data on impact properties and effect of modification are relatively scarce for these alloys. This study focuses on optimization of flow rate of inert gas, starting temperature and duration of gas purging as key GISS parameters in order to obtain most sphericity and grain refinements and also investigate the effect of Sr addition on the microstructural refinement and impact strength of GISS A380 aluminum alloys. The current study tends to improve the existing knowledge on slurry and microstructure formation and mechanical properties of the GISS process.

2 Experimental

2.1 Semi-solid process

In this work, A380 aluminum alloy was used for rheocasting with GISS technique. The chemical composition of this alloy which has been analyzed by a spark emission spectrometer (Hitachi HighTec) is given in Table 1.

Table 1 Chemical composition of A380 alloy (wt.%)

Si	Cu	Fe	Mn	Mg	Zn	Ni	Ti	Al
8.54	2.34	0.23	0.03	0.03	0.3	0.02	0.03	Bal.

In the GISS process, the steps start by having a molten metal with a predetermined amount at a temperature above the liquidus temperature. The flow rate of the inert gas, starting temperature for gas purging or in other words temperature of superheated melt and the duration of gas purging were three key GISS process variables which were changed during this study.

About 500 g of the alloy ingots were melted in

a graphite crucible using an electric resistance furnace. Firstly, the A380 aluminum alloy was melted at the temperature ranging from 700 to 720 °C, and then it was cooled to the chosen pouring temperature (610, 620, 630 and 640 °C) above the liquidus temperature. A thermocouple was used to show the melt temperature. Then, the porous graphite diffuser is immersed, injecting fine argon inert gas bubbles into the melt for holding time of 5, 10, 15 and 20 s until the desired solid fraction is achieved. Consequently, the obtained slurry was poured into a cylindrical metallic die. The flow rate of the argon inert gas was considered as 2 and 4 L/min. The liquidus temperature of this alloy was determined using cooling curve thermal analysis.

Figure 1 shows the sample temperature versus time (the cooling curve) and its first derivative curve of this alloy. Solidification begins with the evolution of heat at the liquidus temperature that leads to a decrease in the cooling rate of the sample. Therefore, a sudden change of slope can be observed on the curve, as shown in Fig. 1. This first intersection of the curves happens at 595 °C, which indicates the liquidus temperature. According to the cooling curve, a drop in temperature of melt was observed simultaneously with the start of the inert gas purging into the melt through the graphite diffuser. As shown, a few seconds after inert gas purging, the melt temperature reached its liquidus temperature. Then, the rate of temperature drop decreased because of latent heat extraction due to α(Al) nucleation. According to CZERWINSKI [24], copious nucleation was induced by the cooling effect of the inert gas bubbles.

Schematic diagram of the process equipment which was used in this study is illustrated in Fig. 2.

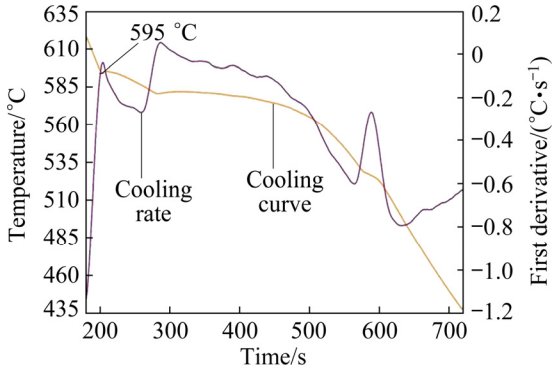

Fig. 1 Cooling curve thermal analysis (CCTA) curve and its first derivative curve of A380 alloy

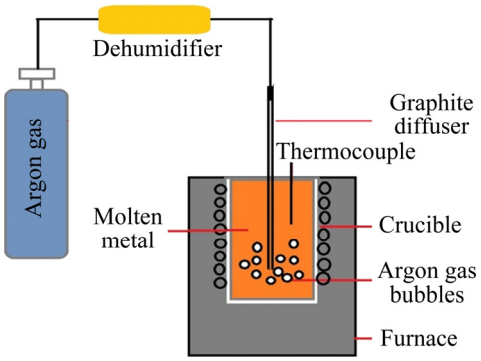

Fig. 2 Schematic of equipment used for GISS process

Moreover, in order to produce an as-cast sample, the melt was poured into a cylindrical metallic mould at 700 °C without performing the GISS process (as-cast).

The GISS optimum conditions to change into globular morphology of α(Al) was studied. Moreover, to study the effect of modification of eutectic silicon, Sr was added to an optimized GISS sample. It was reported that an optimum Sr level is desired to adequately modify the structure, where below a certain level, the eutectic Si is not efficiently modified and above that no additional refinement of the Si morphology happens and porosity formation may occur. It was reported that (200−600)×10^{-6} Sr addition to an Al−7Si−0.5Mg alloy yielded a substantial improvement in elongation [25]. In this study, 0.2 wt.% of Al−10Sr master alloy was wrapped in an aluminium foil, preheated to 200 °C and immersed into the liquid held at (700±10) °C. The liquid was stirred for homogenization about 15 min after addition of Al−10Sr. This sample was then performed by the GISS process and referred to as the GM sample (GISS and modified sample).

2.2 Microstructure observation

GISS samples as well as GM and conventionally cast samples were sectioned and prepared through standard metallography processes and were etched with a 0.5% HF solution. The microstructures were studied by optical microscope. The professional image analysis software (Image-Pro Plus) and linear intercept were adopted to quantify the microstructural features.

Structural evaluation of the samples and fracture surface of specimens was also examined by scanning electron microscopy (SEM, Tescanvega/

XMU, 28 kV) equipped with the energy-dispersive spectroscopy system (EDS).

2.3 Mechanical property tests

The mechanical properties of the produced samples were investigated through hardness and impact strength. The hardness was measured using the MVK−H21 hardness tester. The applied load was 31.25 kg. A total of five measurements were performed on each sample and the average is reported as a hardness value. The impact strength was analyzed by the Charpy impact test. According to ASTM E23 standard, the impact samples were prepared by machining. The Charpy test is the most popular means for laboratory measurement of impact energy. The impact testing equipment allows the fracture response of the impact specimen to be considered in terms of absorbed fracture energy. The fracture surface of specimens was also examined by scanning electron microscopy.

3 Results and discussion

3.1 Microstructural evaluation of as-cast and GISS specimens

The microstructures of as-cast and GISS specimens at the gas flow rate of 4 L/min are shown in Fig. 3 and Fig. 4, respectively. A comparison

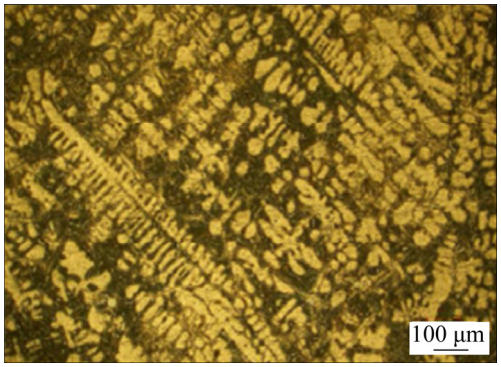

Fig. 3 Microstructure of as-cast specimen

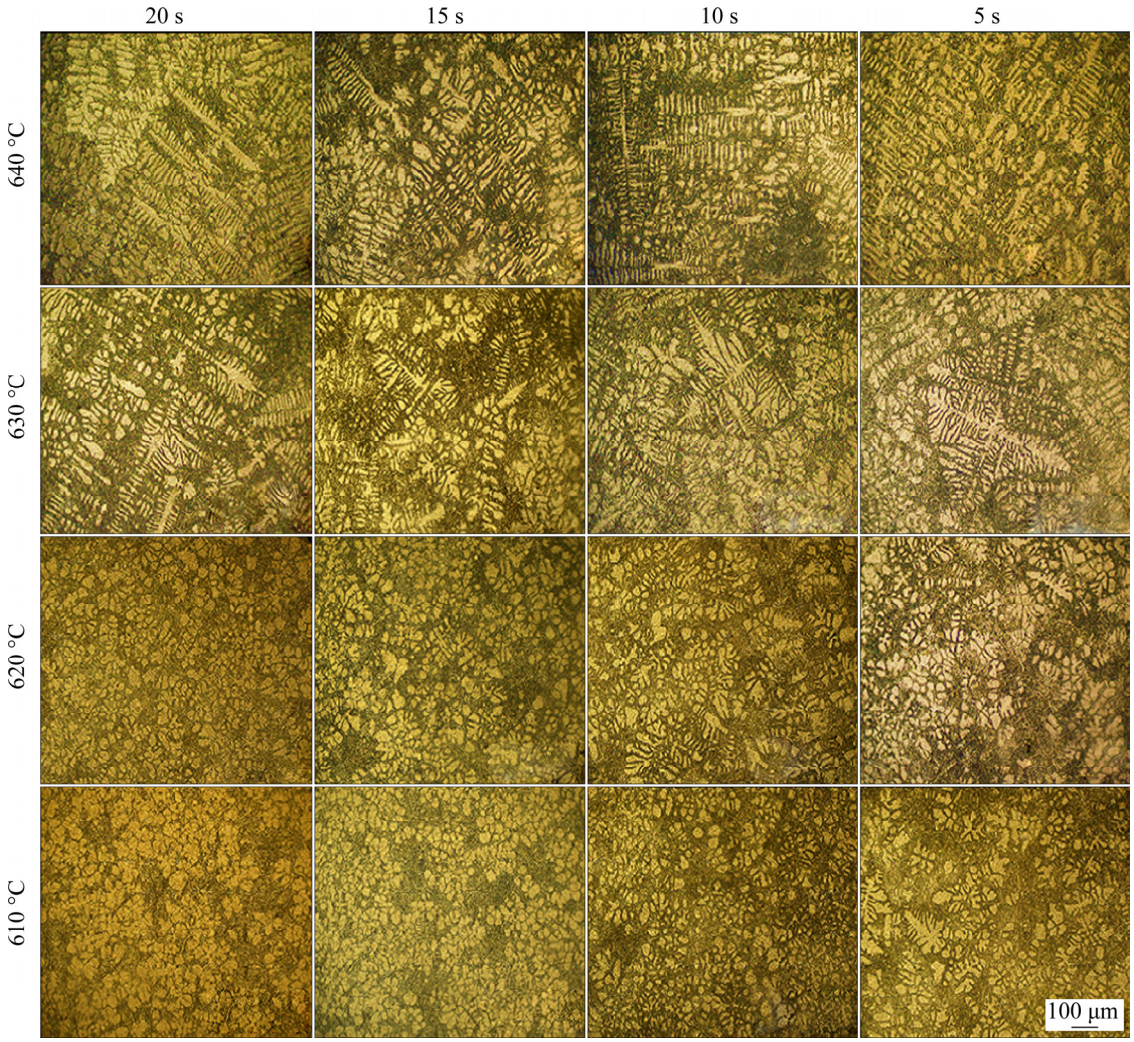

Fig. 4 Microstructures of GISS specimens at gas flow rate of 4 L/min and holding temperatures of 610, 620, 630 and 640 °C for 5, 10, 15 and 20 s

shows that the microstructure of as-cast specimen mainly consisted of large dendritic α(Al) phase (white contrast) surrounded by lamellar eutectic phases containing acicular-like Si particles (dark contrast). However, the GISS casting has finer non-dendritic structure in some conditions. To investigate the influence of pouring temperature and gas purging duration on the microstructure, the molten metal with the temperatures of 640, 630, 620 and 610 °C is poured at the different gas purge durations of 5, 10, 15 and 20 s. There are coarse dendrites and strip-like eutectic silicon in the microstructure of the alloys poured at 640 and 630 °C. As shown, the microstructure of the alloys at temperature of 620 °C for 5 and 10 s consists of majority of finer primary α(Al), a few with a particle-like, and rosette-like morphology. There is not enough time for the dendritic structure to change into the grains with globular morphology, so that the dendritic structure is reserved in the form of rosette-like grains.

As shown in Fig. 4, it can be seen that the morphology of the primary α(Al) changes to rosette, and globular and particle-like grains with decreasing pouring temperature. The globular morphology of the primary α(Al) phase for the GISS specimen is achieved at an holding temperature of 620 °C for 15 and 20 s and at a temperature of 610 °C for 10, 15 and 20 s. The morphology of primary α(A1) changes from rosette to particle-like, and the grain size gradually decreases with the superheat temperature of liquid. When the pouring temperature reaches 610 °C, the morphology of primary α(A1) changes to globular morphology, and there is basically no primary phase with rosette morphology, as shown in Fig. 4. This finer and non-dendritic structure is achieved by the GISS process as reported elsewhere [6,7]. According to Fig. 4, it seems that the most sphericity and grain refinement is achieved at the gas purging temperature of 610 °C for a duration time of 15 s. The optimum amounts of GISS variables were also determined by image analysis to obtain the best globularity in the microstructure of a long freezing range alloy. The exact mechanism of structural formation in the GISS process is still unclear. The likely theory that can explain how a large number of solid particles are formed was proposed by ABDI and SHABESTARI [6]. They reported that a lot of nuclei are formed around graphite diffuser at the early stage of solidification because of the heat extraction effect of the inert gas. These nuclei could be distributed everywhere in the melt and could survive as the temperature dropped to the mushy zone. The agitation due to gas purging causes good uniformity of temperature and composition in the melt. This homogeneity prevents the constitutional undercooling (CUC) and preferred growth of the grains, and therefore multi-directional growth takes places and nuclei develop spherically.

In order to investigate the influence of argon gas flow rate on the microstructure, the molten metal with the optimum temperature of 610 °C is also poured at different gas purging durations of 5, 10, 15 and 20 s and gas flow rate of 2 L/min (Fig. 5). There are coarse dendritic grains and strip-like eutectic silicon in the microstructure of the alloys at gas purging durations of 5 and 10 s (Figs. 5(a, b)). The microstructure of the alloys for 15 and 20 s consists of the majority of rosette primary α(A1) and a few phases with particle-like morphology. Therefore, the flow rate of 2 L/min is not sufficient to change the grains to granular morphology. When gas flow rate decreases from 4 to 2 L/min, the particle size and globularity reduce, which means that the higher the gas flow rate is, the finer and more spherical the primary solid particles are achieved as the result of more uniformity of temperature and composition in the melt.

3.2 Influence of modification with Sr addition

The GISS optimum condition to achieve globular morphology of α(Al) was determined as 610 °C and inert gas injection time of 15 s. The effects of strontium addition on the microstructure of GISS A380 slurries are shown in Fig. 6. Primary silicon in untreated alloy generally has the coarse platelet form with an irregular morphology, as shown in Fig. 3. Small amounts of strontium can change the morphology of the eutectic silicon of Al−Si casting alloys to fine fibrous networks. Addition of modifiers in the form of Al−Sr master alloys is the most simple and efficient process which has been widely used in industry. As shown in Fig. 6, performing the GISS process under the optimum condition on A380 alloy with addition of 0.2% Al−Sr (GM sample), leads to more globular primary α(Al) phase with modified eutectic Si having fibrous microstructure.

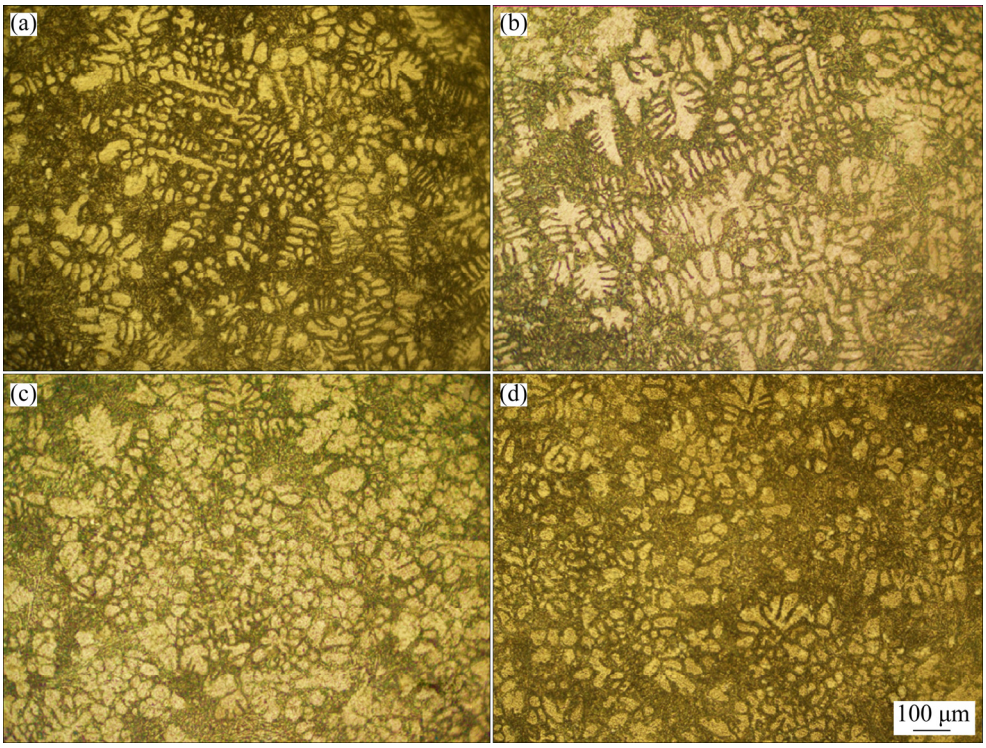

Fig. 5 Microstructures of GISS specimens at gas flow rate of 2 L/min and holding temperatures of 610 °C for 5 s (a), 10 s (b), 15 s (c) and 20 s (d)

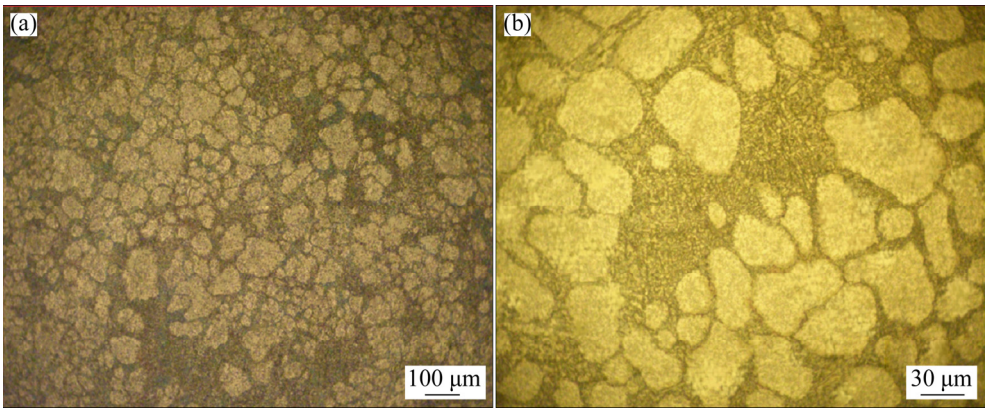

Fig. 6 Microstructure of GM specimen

3.3 Grain size distribution

The operational parameters were also optimized in this investigation by using image analysis in order to obtain a globular microstructure with fine and well distributed α(Al) phase. For this purpose, the influence of gas flow rate, gas purging duration and starting temperature on sphericity, mean particle size and number of mean α(Al) particles per unit area of GISS specimens are illustrated in Fig. 7. The extracted amounts are an average of at least five micrographs related to each sample. The results show that, when argon gas flow rate increases from 2 to 4 L/min, average particle size reduces and the sphericity increases, which means that the higher the inert gas flow rate is, the finer and rounder the primary solid particles are, causing microstructural improvement. Increasing the inert gas flow rate leads to the increase of the rate of heat extraction from the melt, so the driving force for the nucleation is increased and causes the grain size reduction. It is obviously seen that, increasing the starting temperature at a constant gas flow rate leads to the increase in grain size. The parameter of residence time should also be selected in the optimum value. As shown in Fig. 7, increasing the gas purging duration from 5 to 15 s

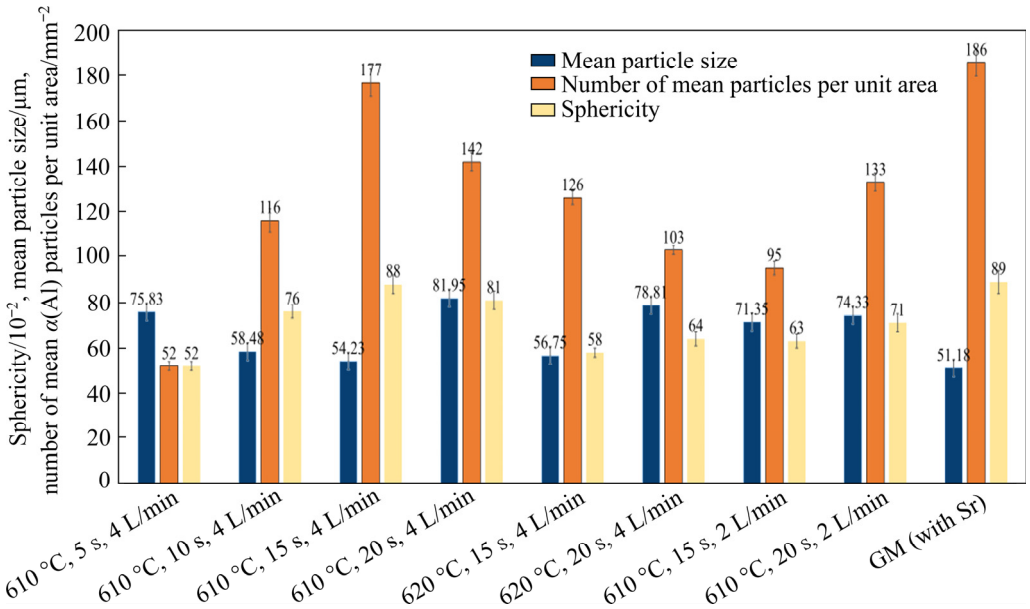

Fig. 7 Sphericity, mean particle size and number of mean α(Al) particles per unit area of GISS specimens at different holding temperatures, durations and inert gas flow rates

at a constant inert gas flow rate and starting temperature leads to the decrease in grain size. Therefore, increasing the copious nucleation in the GISS process is desirable. According to the results, the gas purging duration of 20 s may give an opportunity to the α(Al) and silicon phases to grow.

Image analysis results show that the sphericity of 0.88 and particle size of 54.23 μm were achieved for α(Al) phase in the sample held at 610 °C for 15 s. Also, the number of 177 particles per 1 mm^2 area was obtained in this GISS sample, showing a good distribution of α(Al) phases in the microstructure of the alloy produced by the GISS process. This sample is an optimized GISS sample. Therefore, the starting temperature of 610 °C, the argon gas flow rate of 4 L/min and gas purging duration of 15 s were determined as optimum amounts of the GISS parameters resulting in the most globularity. On the other hand, as shown in Fig. 7, the best sample which has fine grains of 51.18 μm in average size and a high level of globularity of 0.89 was achieved from a GISS processing of Sr modified alloy under optimum conditions which refers to as GM sample.

3.4 Mechanical properties

The morphology of eutectic Si and α(Al) phase plays an important role in determining the mechanical properties of Al−Si alloys. Figure 8 shows the hardness values of as-cast A380, optimized, GM and the sample prepared through GISS at inert gas injection temperature of 610 °C, purging duration of 10 s and flow rate of 4 L/min for comparison. It can be seen that the hardness of as-cast A380 sample is lower than that of GM and GISS samples. The dendritic morphology of the primary phase in the conventionally cast alloys leads to lower mechanical properties of the as-cast sample. The results show that the GISS samples indicate higher value of hardness due to uniform distribution of silicon and α(Al) phases and a reduction in grain size. The hardness of GM (with

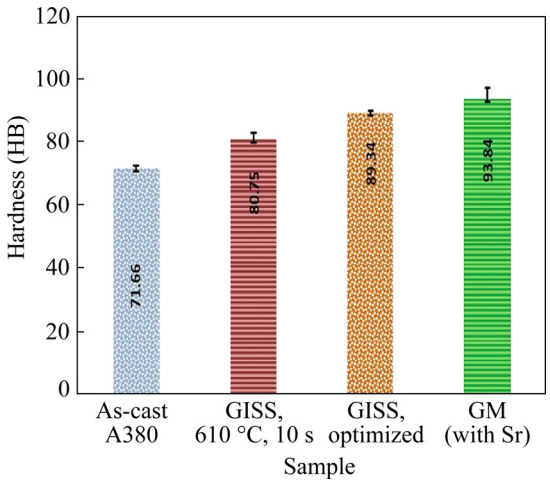

Fig. 8 Hardness of as-cast A380, optimized, GM and sample prepared by GISS at 610 °C for 10 s

Sr) alloy is also increased from (89.34±2.85) to (93.84±3.14) HB for GISS alloys. In the modified GM sample, the microstructure changes from acicular to fibrous silicon, leading to improvement in the mechanical properties. Therefore, the enhanced hardness can be attributed to the presence of the globular structure produced by the unique microstructure obtained by the GISS process and modified eutectic silicon.

The impact strength of as-cast A380, optimized, GM and the sample prepared at inert gas injection temperature of 610 °C, purging duration of 10 s and flow rate of 4 L/min are shown in Fig. 9. As it can be seen, the impact strengths in the as-cast and GISS optimized samples of the A380 alloy are (3.32±0.27) J/cm^2 ((2.77±0.18) J) and (4.67±0.18) J/cm^2 ((4.1±0.21) J), respectively, which show an increase of about 40% due to the globular structure from GISS process leading to improvement of impact strength and ductility. On the other hand, the impact strength of the GM (with Sr) sample, reaches (5.61±0.24) J/cm^2. It is evident from the results that the addition of Sr improves the impact strength of the modified alloy compared to the non-modified alloy. The combination effect of modifying element and the GISS process is a satisfactory operation for obtaining improved microstructure during solidification, and causes the improvement of mechanical properties. The morphology of fibrous Si in Sr-modified alloys enhances toughness because of its important effect on crack initiation and crack propagation resistance. This observation is consistent with that of MOHAMED et al [23], who reported that the combined addition of modifier and grain-refiner to a near eutectic Al−10.8%Si alloy leads to a significant improvement of 33% in impact toughness when compared to the untreated Al−10.8%Si alloy.

The improved mechanical properties, presented in Fig. 9, show the effectiveness of the GISS process and modification. Such enhancement can be attributed to two reasons. One is the refinement of the globular α(Al) in the GISS samples and the presence of fibrous eutectic silicon in the case of the GM sample. According to QI et al [26], fine spherical primary particles are good for rheocasting parts to obtain improved mechanical properties. The strong convection due to enhanced homogeneity in the melt prevents the formation of dendrites and increases the quantity and the globularity of the grains. Moreover, the presence of less shrinkage, porosity and entrapped air due to a higher viscosity and lower casting temperature are the advantages of this process.

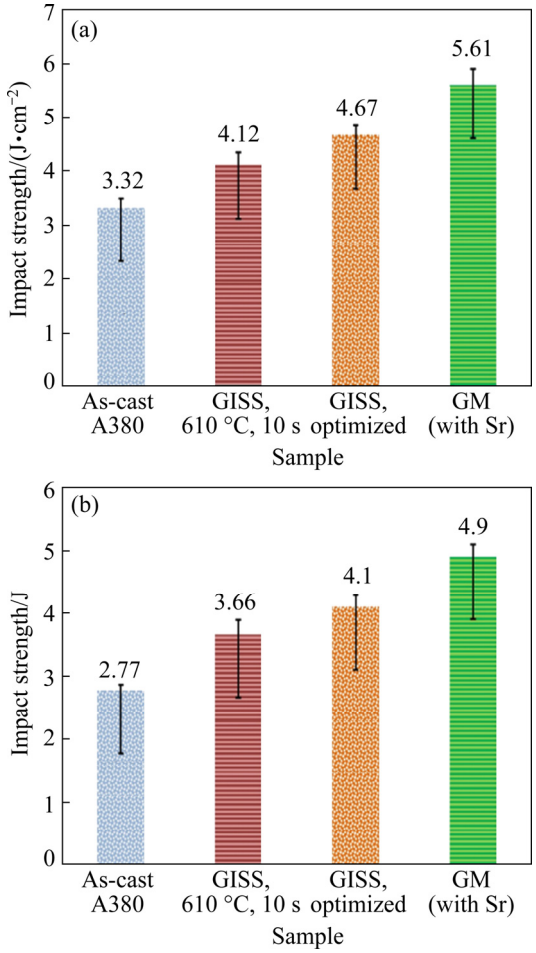

Fig. 9 Impact strength of as-cast, optimized, GM and sample prepared by GISS at 610 °C for 10 s and at 4 L/min

Modification and grain refinement affect not only the total absorbed energy but also the fracture behavior of the impact samples. Figure 10 shows the secondary electron SEM images of fracture surface of as-cast A380, optimized, GM and the sample prepared at inert gas injection temperature of 610 °C, purging duration of 10 s and flow rate of 4 L/min. As seen in Fig. 10(a), fracture surface is large and without any transformation. This means that as-cast specimen has brittle and cleavage fracture. Fracture surfaces of GM (with Sr), optimized and GISS at 610 °C for 10 s specimens are respectively smaller and the number of the surfaces is more than fracture surfaces in as-cast specimen (Figs. 10(b−d)). Fracture surfaces in these

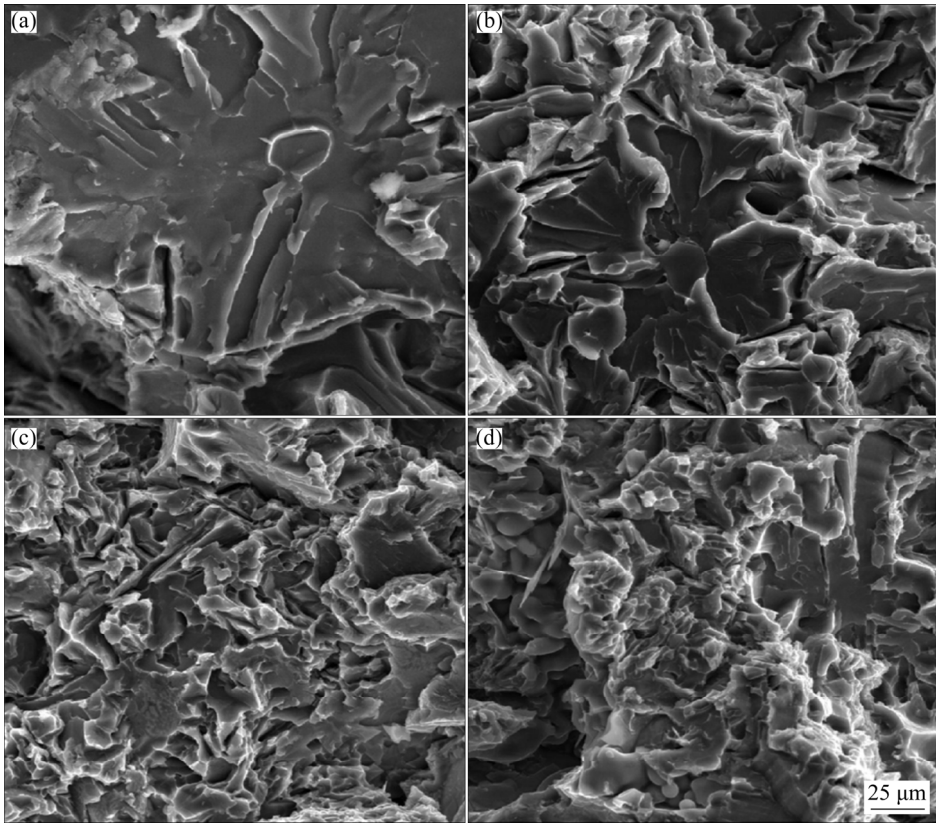

Fig. 10 SE-SEM microstructures of fracture surfaces: (a) As-cast; (b) GISS at 610 °C for 10 s; (c) GISS at 610 °C for 15 s and at 4 L/min; (d) GM (with Sr)

specimens have more transformation because of more ductile aluminium matrix in these specimens. Therefore, the fracture in GISS specimen is mostly ductile. Some tearing edges appear in the fractograph of GISS samples (Figs. 10(b−c)), which shows the characteristic of ductile fracture, and a small smooth region appears. By operating GISS process under optimum condition, the morphology of primary α(Al) changes from coarse dendritic to fine globular, leading to increasing the ductility of aluminium matrix in A380 alloy. On the other hand, the enhancement in mechanical properties observed in GM (with Sr) sample is due to the combination effects of the morphological changes in the shape and size of the silicon particles and fine size of the α(Al) grains caused by GISS and chemical modification processing as compared to the as-cast A380 and GISS alloys.

4 Conclusions

(1) The morphology of primary α(Al) gives priority to rosette-like, and globular-like grains with decreasing pouring temperature. Therefore, most sphericity (0.88) and grain refinement (54.2 μm in particle size) are achieved at the argon gas purging temperature of 610 °C for duration time of 15 s and flow rate of 4 L/min (optimum GISS conditions).

(2) The flow rate of 2 L/min is not capable of changing the grains into the globular morphology. Higher gas flow rate leads to the finer and globular grains.

(3) Addition of strontium leads to the change in the morphology of the eutectic silicon phase to fine fibrous networks. The high level of globularity of 0.89 is achieved from a GISS processing of Sr modified alloy under optimum condition.

(4) The GISS samples indicate higher value of hardness due to uniform distribution of silicon and α(Al) phases and a reduction in grain size with respect to as-cast specimen. The hardness of GM (with Sr) alloy due to fibrous silicon is also increased from (89.34±2.85) to (93.84±3.14) HB for GISS alloys.

(5) The impact strength of the GISS optimized sample due to the globular structure shows an increase of about 40% with respect to as-cast sample. On the other hand, the impact strength

of the GM (with Sr) sample increases to (5.61±0.24) J/cm^2 as the result of the combination effect of modifying element and GISS process in improved microstructure and enhancement of mechanical properties.

(6) The fracture surfaces of GM (with Sr), optimized and GISS at 610 °C for 10 s specimens due to ductile aluminium matrix in these specimens are respectively smaller and the number of the surfaces is more than fracture surfaces in as-cast sample, implying more ductility.

References

[1] GECU R, ACAR S, KISASOZ A, GULER K A, KARAASLAN A. Influence of T6 heat treatment on A356 and A380 aluminium alloys manufactured by thixoforging combined with low superheat casting [J]. Transactions of Nonferrous Metals Society of China, 2018, 28: 385−392.

[2] POLA A, TOCCI M, KAPRANOS P. Microstructure and properties of semi-solid alloys: A literature review [J]. Metals, 2018, 8: 181.

[3] JIANG W M, FAN Z T, CHEN X, WANG B, WU H. Combined effects of mechanical vibration and wall thickness on microstructure and mechanical properties of A356 aluminum alloy produced by expendable pattern shell casting [J]. Materials Science and Engineering A, 2014, 619: 228−237.

[4] MOMENI H, SHABESTARI S G, RAZAVI S H. Densification and shape distortion of the Al−Cu−Mg pre-alloyed powder compact in supersolidus liquid phase sintering process [J]. Iranian Journal of Materials Science and Engineering, 2020, 17: 87−92.

[5] SAHU A, BEHERA A. Semi-solid processing and tribological characteristics of Al−Cu alloy [J]. Materials Today: Proceedings, 2015, 2: 1175−1182.

[6] ABDI M, SHABESTARI S G. Effect of gas induced semi-solid process on solidification parameters and dendrite coherency point of Al−4.3Cu alloy using thermal analysis [J]. Thermal Analysis and Calorimetry, 2019, 136, 6: 2211−2220.

[7] ABDI M, SHABESTARI S G. Semi-solid slurry casting using gas induced semi-solid technique to enhance the microstructural characteristics of Al−4.3Cu alloy [J]. Solid State Phenomena, 2019, 285: 253−258.

[8] KIRKWOOD D H, SUERY M, KAPRANOS P, ATKINSON H V, YOUNG K P. Semi-solid processing of alloys [M]. New York (NY): Springer Series in Materials Science, 2009.

[9] HU X G, ZHU Q, ATKINSON H V, LU H X, ZHANG F, DONG H B, KANG Y L. A time-dependent power law viscosity model and its application in modelling semi-solid die casting of 319s alloy [J]. Acta Materialia, 2017, 124: 410−420.

[10] QU W Y, LUO M, GUO Z P, HU X G, ZHANG A, ZHANG F, LU H X, ZHANG Y Z, LI D Q. Microstructural evolution mechanism of semi-solid slurry: A study using Phase-Field-Lattice-Boltzmann scheme [J]. Journal of Materials Processing Technology, 2020, 280: 116592.

[11] LIU Z Y, MAO W M, WANG W P, ZHENG Z K. Preparation of semi-solid A380 aluminum alloy slurry by serpentine channel [J]. Transactions of Nonferrous Metals Society of China, 2015, 25: 1419−1426.

[12] WANNASIN J, MARTINEZ R A, FLEMINGS M C. Grain refinement of an aluminum alloy by introducing gas bubbles during solidification [J]. Scripta Materialia, 2006, 55: 115−118.

[13] WISUTMETHANGOON S, THONGJAN S, MAHATHANINWONG N, PLOOKPHOL T, WANNASIN J. Precipitation hardening of A356 Al alloy produced by gas induced semi-solid process [J]. Materials Science and Engineering A, 2012, 532: 610−615.

[14] WANNASIN J, JANUDOM S, RATTANOCHAIKUL T, CANYOOK R, BURAPA R, CHUCHEEP T, THANABUMRUNGKUL S. Research and development of gas induced semi-solid process for industrial applications [J]. Transactions of Nonferrous Metals Society of China, 2010, 20(S3): s1010−s1015.

[15] RATTANOCHAIKUL T, JANUDOM S, MEMONGKOL N, WANNASIN J. Development of aluminum rheo-extrusion process using semi-solid slurry at low solid fraction [J]. Transactions of Nonferrous Metals Society of China, 2010, 20: 1763−1768.

[16] CHUCHEEP T, BURAPA R, JANUDOM S, WISUTMETHANGOON S, WANNASIN J. Semi-solid gravity sand casting using gas induced semi-solid process [J]. Transactions of Nonferrous Metals Society of China, 2010, 20(S3): s981−s987.

[17] FLEMINGS M C. Solidification processing [J]. Metallurgical Transactions, 1974, 5: 2121−2134

[18] FAN Z, FANG X, JI S. Microstructure and mechanical properties of rheo-diecast (RDC) aluminium alloys [J]. Materials Science and Engineering A, 2005, 412: 298−306.

[19] JK S, FAN Z. Solidification behavior of Sn−15 wt pct Pb alloy under a high shear rate and high intensity of turbulence during semisolid processing [J]. Metallurgical and Materials Transactions A, 2002, 33: 2002−3511.

[20] DAHLE A K, NOGITA K, MCDONALD S D, DINNIS C, LU L. Eutectic modification and microstructure development in Al−Si alloys [J]. Materials Science and Engineering A, 2005, 413/414: 243−248.

[21] CHEN Zheng-zhou. Preparation of semi-solid A356 Al-alloy slurry by introducing grain process [J]. Transactions of Nonferrous Metals Society of China, 2012, 22: 1307−1312.

[22] TIMPEL M, WANDERKA N, SCHLESIGER R, YAMAMOTO T, LAZAREV N P, ISHEIM D, SCHMITZ G, MATSUMURA S, BANHART J. The role of strontium in modifying aluminium–silicon alloys [J]. Acta Materialia, 2012, 60: 3920−3928.

[23] MOHAMED A M A, SAMUEL F H, SAMUEL A M, DOTY H W. Influence of additives on the impact toughness of Al−10.8%Si near-eutectic cast alloys [J] Materials & Design, 2009, 30: 4218−4229.

[24] CZERWINSKI F. Modern aspects of liquid metal engineering [J]. Metallurgical and Materials Transactions B, 2017, 48: 367−93.

[25] ZAMANI M, SEIFEDDINE S. Determination of optimum Sr level for eutectic Si modification in Al−Si cast alloys using thermal analysis and tensile properties [J] International Journal of Metalcasting, 2016, 10: 457−465.

[26] QI M F, KANG Y L, ZHOU B, LIAO W N, ZHU G M, LI Y D, LI W R. A forced convection stirring process for Rheo-HPDC aluminum and magnesium alloys [J]. Materials Processing Technology, 2016, 234: 353−367.

气体诱导半固态加工和添加 Sr 对 A380 铝合金冲击强度和组织细化的影响

M. HONARMAND, M. SALEHI, S. G. SHABESTARI, H. SAGHAFIAN

School of Metallurgy and Materials Engineering,
Iran University of Science and Technology (IUST), Narmak, Tehran, Iran

摘　要：采用气体诱导半固态(GISS)加工工艺制备 A380 铝合金， 研究氩气惰性气体流量、起始温度和气体吹扫时间等 GISS 关键参数以及 Sr 改性对合金的组织细化、硬度和冲击强度的影响。显微组织演化表明，浇铸时间和 Sr 添加对合金中初生 α(Al)的形貌和尺寸有较大影响，使其由粗大的枝晶状组织转变为细小的球形组织。对 Sr 改性合　金进行 GISS 加工，当气体注入的起始温度为 610 ℃时，获得具有平均晶粒尺寸为 51.18 μm、高球形度(0.89)细晶组织的最优样品。与铸态样品相比，GISS 加工获得的最优样品由于球形组织和 Si 的纤维状形貌，其冲击强度((4.67±0.18) J/cm^2)提高约 40%；而且，Sr 改性和 GISS 加工使合金的硬度从(89.34±2.85) HB 提高到(93.84±3.14) HB。Sr 改性合金的断裂面以复杂形貌为主，具有典型的韧性断裂特征。

关键词：气体诱导半固态加工；冲击强度；A380 铝合金；球形组织；改性

(Edited by Bing YANG)